Modeling the interactions of phthalocyanines in water: From the Cu(II)-tetrasulphonate to the metal-free phthalocyanine

Elisa I. Martín, Jose M. Martínez, and Enrique Sánchez Marcos[a)]
Departamento de Química Física, Universidad de Sevilla, E-41012 Sevilla, Spain

(Received 17 August 2010; accepted 30 November 2010; published online 10 January 2011)

A quantum and statistical study on the effects of the ions Cu^{2+} and SO_3^- in the solvent structure around the metal-free phthalocyanine (H_2Pc) is presented. We developed an *ab initio* interaction potential for the system CuPc–H_2O based on quantum chemical calculations and studied its transferability to the H_2Pc–H_2O and $[CuPc(SO_3)_4]^{4-}$–H_2O interactions. The use of the molecular dynamics technique allows the determination of energetic and structural properties of CuPc, H_2Pc, and $[CuPc(SO_3)_4]^{4-}$ in water and the understanding of the keys for the different behaviors of the three phthalocyanine (Pc) derivatives in water. The inclusion of the Cu^{2+} cation in the Pc structure reinforces the appearance of two axial water molecules and second-shell water molecules in the solvent structure, whereas the presence of SO_3^- anions implies a well defined hydration shell of about eight water molecules around them making the macrocycle soluble in water. Debye–Waller factors for axial water molecules have been obtained in order to examine the potential sensitivity of the extended x-ray absorption fine structure technique to detect the axial water molecules. © *2011 American Institute of Physics*. [doi:10.1063/1.3528934]

I. INTRODUCTION

Photodynamic therapy (PDT) is an emerging noninvasive binary therapy for the treatment of different types of cancers. It involves the use of a photosensitizer (PS) in combination with visible light to produce reactive oxygen species which selectively destroy malignant cells.[1–4] A large number of metal-containing macrocycles have been synthesized and investigated for application in PDT, since the first approval of hematoporphyrin derivatives as a PS for PDT clinical applications.[5–9]

Among many important technological applications,[10–13] phthalocyanines (Pcs) have been recently identified as promising PSs for PDT because their typical absorption at ~ 680 nm is more intense than that corresponding to the porphyrin family.[14] However, Pcs are generally known to be insoluble due to their strong tendency to aggregate in aqueous solutions because of their high lattice energy.[15–18] Both properties can significantly decrease their photosensitizing ability. Besides, water solubility is an essential requirement for PDT action.[19]

In order to decrease Pc aggregation and increase their photodynamic activity, apart from metal and metalloid atoms inserted in the macrocycle center to substitute the two central hydrogen atoms of metal-free phthalocyanine (H_2Pc), several hydrophilic and amphiphilic groups have been introduced in the macrocycle periphery obtaining different substituted and soluble metal phthalocyanines (MPcs).[5,20]

There is a significant number of studies which present the photochemical and electronic properties of metal-free phthalocyanines and their substituted or nonsubstituted metal derivatives.[21–25] However, none of them have dealt with the basic interactions of these derivatives with water which are finally responsible for their solubility. Thus, the solvent structure around these compounds in water and the influence of the metal cation in the central cavity as well as hydrophilic and amphiphilic groups at the macrocycle periphery have not been investigated at a theoretical level. In order to address this question, this work is devoted to the theoretical study by means of classical molecular dynamics (MD) simulations of a set of three representative phthalocyanine derivatives in water. This will supply a molecular description of the main factors determining the interactions of water molecules with the different chemical motifs belonging to the macrocycle.

In this case, we have chosen the CuPc complex which is the most common metal phthalocyanine produced and used in the industry. This complex is a macrocyclic conjugated planar molecule formed by four isoindole units, joined by four nitrogen atoms, rendering a unique fully symmetric tetradentate ligand [Fig. 1(a)]. Although CuPc is a rather large complex, it is quite rigid, probably due to the so-called macrocyclic effect which yields, for a complex with a cyclic polydentate ligand, a greater stability than for a comparable noncyclic ligand. This fact allows us to treat the copper complex as rigid when studying the CuPc–H_2O interaction, in contrast to other biochemical metal environments, where the inherent flexibility of the peptide units must be taken into account.[26] In order to study the effects of Cu^{2+} cation in the macrocyle and the $(SO_3)^-$ anions in the hydration structure, the metal-free phthalocyanine (H_2Pc) [Fig. 1(b)] and the 3,4′ ,4′′ ,4′′′-tetrasulphonated derivative of the CuPc complex, $[CuPc(SO_3)_4]^{4-}$ [Fig. 1(c)] have also been investigated. The comparison among the three types of structures will allow us to get insight in their different interactions with water as well as to monitor the changes from unsoluble to soluble behaviors.

The first step in this work is the development of an appropriate intermolecular potential between the CuPc complex and water. We have taken advantages of some of our previous

a)Electronic mail: sanchez@us.es.

 © 2011 American Institute of Physics

Author complimentary copy. Redistribution subject to AIP license or copyright, see http://jcp.aip.org/jcp/copyright.jsp

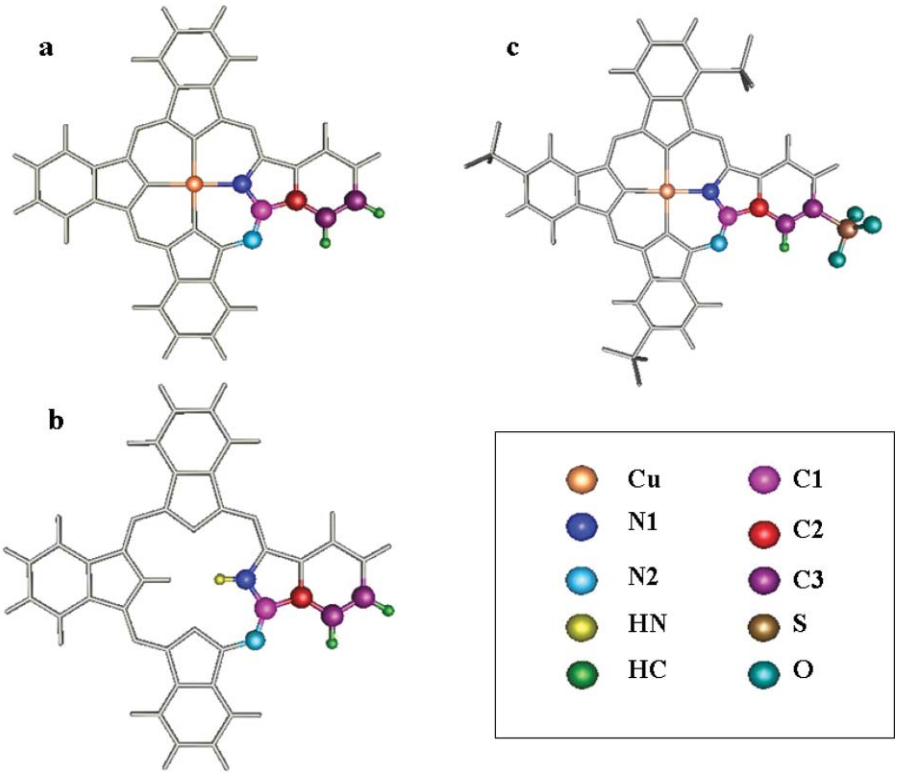

FIG. 1. Structure and atomic types employed for the three phthalocyanines studied: (a) CuPc, (b) H_2Pc, and (c) $[CuPc(SO_3)_4]^{4-}$.

strategies for developing hydrated ion–water interaction potentials, based on the hydrated ion model, $[M(H_2O)_x]^{n+}$ and *ab initio* quantum–mechanical interaction energies.[27–29] In the current case, the metal cation, Cu^{2+} is coordinated to a Pc^{2-} macrocycle, the solvent interacting with the complex by means of an *ab initio* MPc–H_2O interaction potential. Therefore, the role played by the water molecules of the first shell in the metal aquaion, $(H_2O)_x$, is now played by the macrocycle, Pc^{2-}.

The paper is organized in the following manner. The development of an *ab initio* interaction potential for CuPc–H_2O is presented and tested by carrying out classical MD simulations. The degree of transferability of this interaction potential to the other two Pcs is investigated, and the corresponding intermolecular potentials are established and tested for H_2Pc–H_2O and $[CuPc(SO_3)_4]^{4-}$–H_2O. Energetic and structural properties are extracted from the analysis of these simulations and differences among them are highlighted.

II. METHODOLOGY

The lack of interaction potentials suitable for describing the hydration phenomenon of phtalocyanine complexes forces us to develop them as a first step in this study. In this section, the building process of *ab initio* interaction potentials between each of the three different macrocyclic compounds (CuPc, H_2Pc, and $[CuPc(SO_3)_4]^{4-}$) and the solvent is described together with the molecular dynamics simulation details. Two different strategies have been followed in the potential development. The first potential built corresponds to the CuPc complex and it is based on a thorough exploration of the potential energy surface (PES) involving the complex and a water molecule. An analytical site–site-like function is then used to describe the interaction between the two units. A set of coefficients present in the mathematical expression are fitted to reproduce the quantum interaction energies. The other two potentials are built on the basis of an extension of the CuPc–H_2O potential, transferability playing a key role in the development process.

A. CuPc–H_2O interaction potential

A set of quantum–mechanical interaction energies must be computed to define an *ab initio* based interaction potential like those presented in this work. It implies the definition of the level of calculation and the way the PES is sampled in order to extract representative configurations. In the next two sections both aspects are considered.

1. Quantum chemical computations: Choice of the level of calculation

In order to make computations affordable, considering the size of the complexes we are dealing with and the number of calculations needed to develop the first of the interaction potentials (CuPc–water), a compromise between accuracy and feasibility must be accepted. For that reason a much smaller system is used in test calculations. The reference complex must have a similar environment to that found for copper atom in the phthalocyanine, i.e., a neutral complex with a

Author complimentary copy. Redistribution subject to AIP license or copyright, see http://jcp.aip.org/jcp/copyright.jsp

planar coordination environment for the cation defined by four nitrogen atoms. The $Cu(NH_3)_2$ $(NH_2)_2$ complex fulfills those requirements and has been used for that purpose, optimizing a C_{2v} structure under the constraint of fixing the Cu and the four N atoms within the same plane (See Table 1S in the supplementary material).[30] The fully relaxed structure is only 2.9 kcal/mol more stable than the C_{2v} structure here used. The CuPc complex is a neutral open-shell system, whose most stable electronic state is a doublet, the radical character mainly associated to the Cu $3d_{x^2-y^2}$ orbital, which overlaps the Cu–N bond regions in the molecular plane, with small contributions from the in-plane 2p orbitals of the ligand atoms.[31] The model complex, $Cu(NH_3)_2(NH_2)_2$, is also a neutral open-shell system, where the most stable electronic state is also a doublet. As in the case of the CuPc complex, the highest spin density is associated to the Cu $3d_{x^2-y^2}$ orbital with small contributions from the in-plane N 2p orbitals of the amino-ligands.

The model complex and a water molecule have been optimized at different level of computations employing the 6-31g(d) basis set and keeping those geometries fixed, the intermolecular Cu–O distance has been optimized along the axial direction. The *ab initio* calculations have been performed with the GAUSSIAN 03 package.[32] For each case, the interaction energy at those geometries, defined as

$$E_{\text{int}} = E_{\text{Cu(NH}_3)_2(\text{NH}_2)_2-\text{H}_2\text{O}} - E_{\text{Cu(NH}_3)_2(\text{NH}_2)_2} - E_{\text{H}_2\text{O}}, \quad (1)$$

has been computed. Table I collects those results.

As a reference method, Table I also contains CCSD single point calculations for the optimized geometries. Among the four methods, BHLYP provides the closest results to those of the CCSD level and is therefeore adopted for obtaining the interaction energies between the phthalocyanine complexes and the solvent. Previous works on Cu(II) complexes[33,34] also shows the suitability of this functional when compared with CCSD(T) results.

The proper use of a pure *ab initio* based two-body potential implies that many-body effects[35] must be small enough (approximately negligible) in order to approximate the total interaction energy as a sum of pair interactions (pairwise additivity approximation). Potentials were fitted to the *ab inito* interaction energies without including BSSE (basis sets superposition error) corrections, following a recent study of Alvarez-Idaboy and Galano.[36] which suggests that when small basis sets are used the application of the counterpoise method worsens the noncorrected interaction energies compared to the CBS-extrapolated results. The use of a rather small basis sets is imposed by the large computational cost needed to obtain the fitted potentials. Two factors are responsible of these high requirements. The quite large size of the solute molecule and the high number of configurational arrangements needed for an appropriate potential energy surface scan. Following the strategy of Kim *et al.*[37] for the BSSE estimation of the interaction energy, the most attractive configuration found in the scan has a relative error of 30%. This should be considered a reasonable upper limit for the error estimation because the considered structure is one of the arrangement where the fragments are closer. Once provided the feasibility of the methodology for building this type of intermolecular potentials, additional computational efforts will be made to improve the quantum-mechanical level.

TABLE I. Optimized Cu–O distance and interaction energies for the $[Cu(NH_3)_2(NH_2)_2–H_2O]$ complex at different levels of calculation. Values in parenthesis correspond to the single point CCSD interaction energies computed at optimized geometries of the different methods. Distances are in Å and energies in kcal/mol.

	HF	B3LYP	BHLYP	MP2
$\mathbf{r}_{\text{Cu–O}}$	2.52	2.52	2.43	2.42
$\mathbf{E}_{\text{int}}$	–2.23	–2.42	–3.51	–4.16
	(–3.65)	(–4.49)	(–3.83)	(–3.47)

Before sampling the PES of the CuPc–H_2O system with the aim of developing the corresponding interaction potential, a test exploration has been performed in order to detect possible many-body effects appearing when more than one water molecule simultaneously interacts with the target complex. In this context, polarization effects present in a metal center simultaneously interacting with two water molecules have been previously detected in square planar complexes of Pt(II) (Ref. 38) leading to asymmetric solvation environments around the metal ion. With that purpose a set of geometries in which two water molecules located in the axial region above and below the molecular CuPC plane have been tested. One of the water molecules is kept fixed at a distance that optimizes the interaction with the copper complex (2.66 Å), while the second solvent molecule (on the other side of the molecular plane) is moved along the axial direction as shown in Fig. 2. For each of the considered geometries, the total interaction energy is defined as

$$E_{\text{int}} = E_{\text{CuPc(H}_2\text{O})_2} - E_{\text{CuPc}} - 2E_{\text{H}_2\text{O}} \quad (2)$$

and can be compared with the equivalent quantity assuming pairwise additivity,

$$E_{\text{int}}^{\text{two-body}} = E_{\text{int}}(\text{CuPc(H}_2\text{O})_A) + E_{\text{int}}(\text{CuPc(H}_2\text{O})_B) + E_{\text{int}}(\text{H}_2\text{O}_A - \text{H}_2\text{O}_B). \quad (3)$$

The different E_{int} appearing on the right hand side of Eq. (3) are defined as in Eq. (1). Figure 2 shows the excellent agreement between energies obtained through expressions (2) and (3) revealing how, in this case, the interaction with one water molecule in the neighborhood of the metal center does not alter significantly the interaction of the complex with a second water molecule located on the other side of the molecular plane. These results are reasonable to adopt a pure two-body approximation when building a CuPc–H_2O interaction potential.

2. PES exploration and potential building

Compared to previous pair interaction potentials involving smaller metal ion complexes, the size of the CuPc complex forces now to a much larger exploration of the PES. Due to the symmetry of the complex, only half of the two hemispheres around the complex has to be sampled. Figure 3 shows the polar coordinates employed for the

Author complimentary copy. Redistribution subject to AIP license or copyright, see http://jcp.aip.org/jcp/copyright.jsp

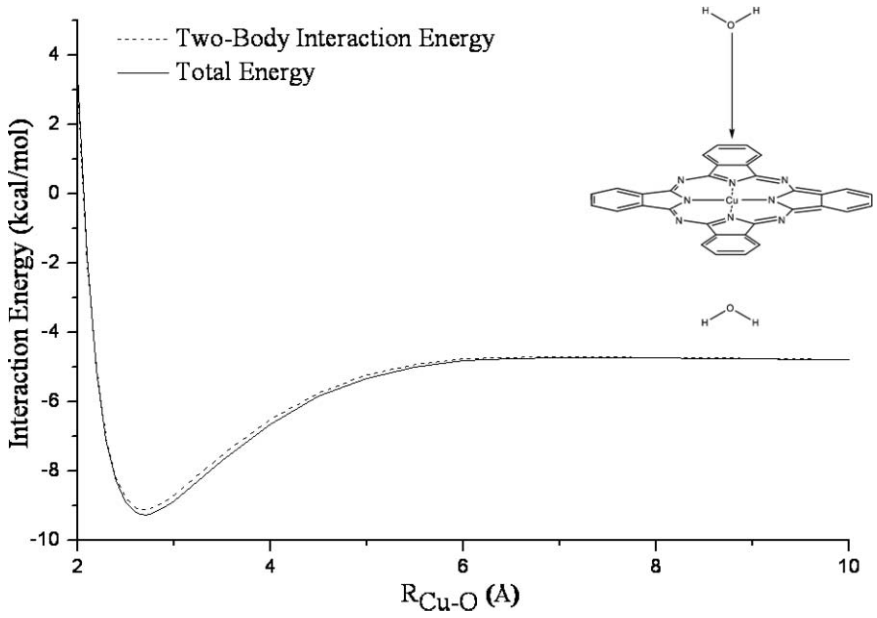

FIG. 2. Total and two-body interaction energy obtained through expressions (2) and (3).

surface prospection and Table II, the ranges and steps employed for the three variables.

Additionally, different orientations of the water molecule were also sampled. Specifically, three orientations have been considered and are also shown in Fig. 3. They correspond to ion–dipole, inverse ion–dipole, and hydrogen bond like orientations. This systematic prospecting produced more than 2200 single point calculations from which the interaction energies were computed. It is worth mentioning that the internal water geometry is kept fixed and consistent with the water model to be employed in the molecular dynamics simulations, i.e., the SPC/E model.[39]

To describe the interaction between the CuPc complex and the solvent during the molecular dynamics simulations

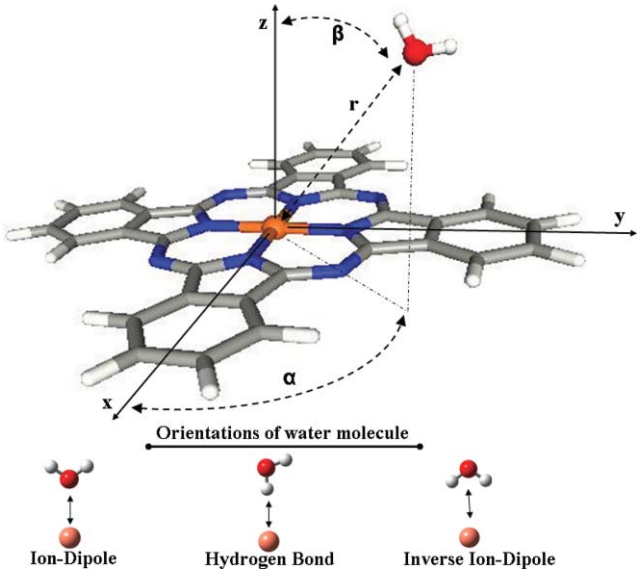

FIG. 3. Coordinates and orientations employed in the exploration of the CuPc–H_2O PES.

the following site–site type analytical function has been employed:

$$E_{\mathrm{CuPc-H_2O}} = \sum_{\mathrm{i}}^{\text{CuPc sites}} \sum_{\mathrm{j}}^{\text{water sites}} A_{\mathrm{ij}} \cdot e^{-\mathrm{B}\cdot \mathrm{r_{ij}}} + \frac{C_6^{\mathrm{ij}}}{\mathrm{r}_{\mathrm{ij}}^6} + \frac{D_8^{\mathrm{ij}}}{r_{\mathrm{ij}}^8} + \frac{E_{10}^{\mathrm{ij}}}{\mathrm{r}_{\mathrm{ij}}^{10}} + \frac{q_i q_j}{r_{\mathrm{ij}}}. \quad (4)$$

Charges present in the electrostatic contribution to the interaction have been obtained by means of the Merz–Kollman procedure[40,41] (BHLYP/6-31g(d) calculation of the CuPc system). The SPC/E charges have been used for the water atoms. Parameters present in the short range terms (exponential and r^{-n} contributions) have been fitted to reproduce the whole set of interaction energies. Different sets of exponents, n, were tried during the fitting process, the 6-8-10 combination providing the best fit. The common employed 6-12 functional form leads to a fitting much less satisfactory what indicates the complexity of the short-range interactions in the region close to the macrocycle. Potential function must keep the symmetry of the units, in particular that present in the phthalocyanine complex, thus atoms have been grouped according to the chemical nature and symmetry. The labels employed are shown in Fig. 1(a), and Table 2S in the supplementary material[30] lists all the fitted coefficients and charges employed in expression (4). The fit quality is shown in Fig. 4 where the fitted energies are plotted against the *ab initio* interaction energies. A standard deviation of 0.63 kcal/mol is obtained showing the excellent correlation between the quantum chemical information and the analytical function employed to describe the CuPc–solvent interaction.

In spite of the large number of geometries considered in the fitting process, the complexity of the copper phthalocyanine system compelled us to explore in detail the behavior of expression (4) for the geometries not included in the set of points used during the fitting process. The aim is to

Author complimentary copy. Redistribution subject to AIP license or copyright, see http://jcp.aip.org/jcp/copyright.jsp

TABLE II. Ranges and steps employed for the three variables in the exploration of the CuPc-H_2O PES.

Variable	Range	Step
r (Å)	1.4–7.4	0.1–0.25
α (°)	0–45	9
β (°)	0–80	10

discard anomalous or strange results for unexplored regions by means of building up isocontour maps in which a systematic sampling of a water molecule position is performed optimizing its orientation at each point. Figure 5 shows one of those plots in which the oxygen of the probe water is kept in a plane distant 2 Å from the CuPc plane. An appropriate behavior (no artificial holes—deep attractive wells—or peaks—high repulsive barriers) together with the right symmetry of the interaction can easily be observed, what supposes an additional validation of the developed interaction potential.

B. Extending the CuPc–H_2O interaction potential to other phtalocyanine complexes

Taking into account the chemical similarities among the CuPc, H_2Pc, and $[CuPc(SO_3)_4]^{4-}$ complexes and the high computational cost needed to develop the CuPc–water interaction potential, it would be desirable to follow a cheaper strategy when describing the interaction with the solvent molecules for the other two cases. The strategy adopted relies on the possibility of making part of the CuPc–water potential transferable to the other complexes, fact likely feasible, due to the limited chemical changes present when moving from one compound to another. From a practical point of view, it means to keep partly the short-range contribution of the interaction potential (r^{-n} terms) by maintaining the coefficients fitted in the CuPc case for most of the atoms also present in the new complexes. The coefficients associated only to the chemically different groups can be obtained either by a fitting process or by adopting, if available, a functional form and associated coefficients already published in the literature. The first option has been employed in the H_2Pc complex, because as in the copper complex no information is available for that system in terms of interaction potentials. However, for the sulphonated derivative, Lennard-Jonnes type parameters are available[42] in the literature for the SO_3^- unit. We have adopted them and coupled with the rest of the parameters developed for the CuPc system. In this case, however, the system presents some extra degrees of freedom associated to the rotation of the sulphonate units.

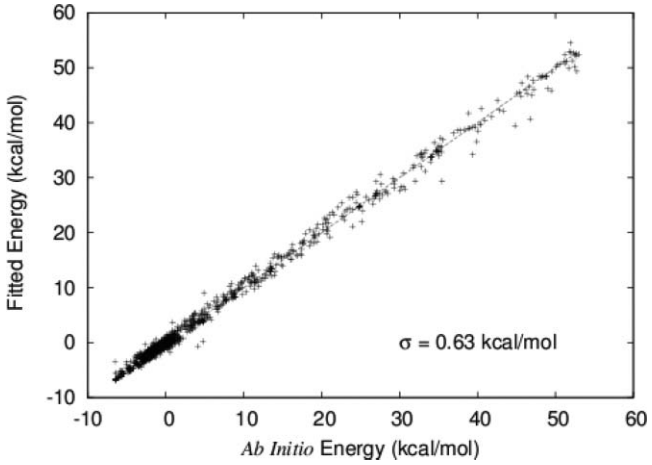

FIG. 4. Fitted vs *ab initio* energy for the CuPc–H_2O interaction.

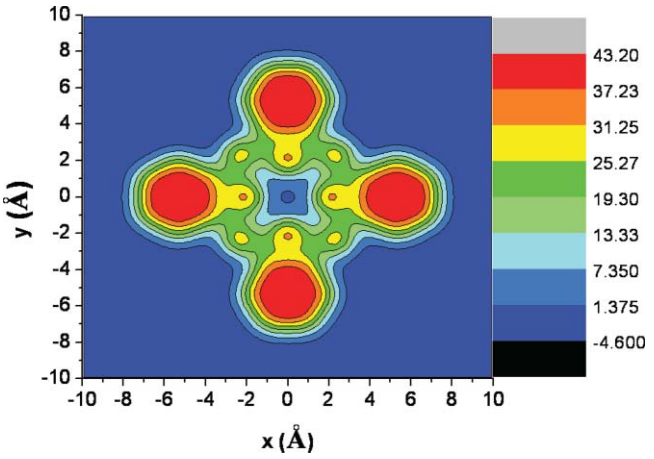

FIG. 5. Isoenergetic contour for the CuPc–H_2O interaction for the plane $z = 2$ Å. The CuPc system is in the plane xy. Energy values are in kcal/mol.

The electrostatic contribution to the interaction energy is adapted to each of the complexes following the same procedure employed in the CuPc case: a set of charges reproducing the electrostatic potential generated by the converged wavefunction at the optimized geometry of the complex. The level of calculation in the two new cases is the same as that previously used for the CuPc system. Opposite to the short-range contributions, the electrostatic part is then specifically obtained for each complex but at a very low computational effort: a single quantum chemical calculation provides all the formal charges needed for that contribution.

1. The H_2Pc–H_2O case

Figure 1(b) shows the atomic types used in the definition of the H_2Pc complex. Compared to the CuPc complex, only the central part of the macrocycle changes: the tetracoordinated copper cation is now substituted by two hydrogen atoms linked to two of the four previously defined N1 type nitrogen atoms.

In our approach, the short-range coefficients associated to the two hydrogen and four nitrogen atoms nearest to the center of the complex will be now fitted by performing a PES survey. At first glance, it could be reasonable to explore only the region around the center of the macrocycle because that is where the new involved atoms are located. However, in order to check our strategy involving transferability, a full scan similar to that performed in the CuPc case has been performed. In this way we do not only sample the right region for fitting the new coefficients but also generate information useful to check the quality of the approximation. The set of coefficients obtained from the fitting and charges are shown in Table 3S in

Author complimentary copy. Redistribution subject to AIP license or copyright, see http://jcp.aip.org/jcp/copyright.jsp

the supplementary material.[30] The goodness of fitting can be observed in Fig. 6, showing the excellent agreement between the *ab initio* and the fitted interaction energies. In fact, the standard deviation remains below 1 kcal/mol what undoubtedly supports the strategy followed to generate a H_2Pc–H_2O interaction potential based on the one previously developed for the copper complex. This agreement is a relevant achievement concerning future works because we have at our disposal a valid strategy for building lower cost interaction potentials for other metal–phatolocyanine complexes.

2. The $[CuPc(SO_3)_4]^{4-}$–H_2O case

The transition from the CuPc to the tetrasulphonated copper macrocycle interaction potential has been done adopting the CHARMM (Ref. 42) Lennard-Jones parameters for the S and O atoms of the SO_3^- units (see Table 4S in the supplementary material[30]). For the rest of atoms, the short range parameters of the CuPc complex have been kept. The $[CuPc(SO_3)_4]^{4-}$ charges are showed in Table 5S in the supplementary material.[30]

In this case, we have tested the approximation by means of comparing *ab initio* interaction energies and energies obtained by the analytical potential for structures involving water molecules around the sulphonates groups generated from a molecular dynamics simulation. A set of 615 structures have been considered and the standard deviation obtained is 3.8 kcal/mol. Although the σ value is larger for this complex, we have to take into account that in this case, the average interaction energy of water molecules in the neighborhood of the sulphonate groups is about 3-fold larger than in the previous complexes, due to the net charge introduced by each sulphonate. Thus, the relative error of the approach can still be considered acceptable.

A difficulty found when introducing the SO_3^- groups is their ability to rotate. In order to take into account that possibility, a rotational barrier has been introduced by fitting a torsional potential to the quantum chemical energies obtained when rotating the groups. The $[CuPc(SO_3)_4]^{4-}$ complex presents two nonequivalent sulphonate groups, see Fig. 1(c). For the three equivalent units (linked to carbon 4), a rotation barrier of 1.7 kcal/mol is found, whereas in the nonequivalent unit (linked to carbon 3) this barrier reaches 7.6 kcal/mol. A cosine function, typically used in torsional barriers ($E_{tor} = V_n[1 + \cos(n\phi - \delta)]$), has been fitted in each case to reproduce the rotation energy profiles.

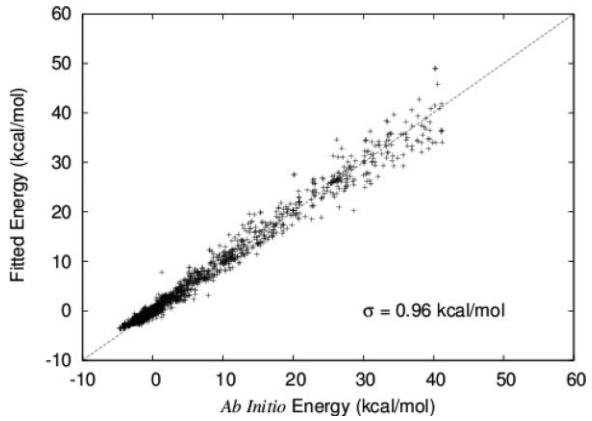

FIG. 6. Fitted vs *ab initio* energy for the H_2Pc–H_2O interaction.

C. Simulation details

Molecular dynamics simulations at 300 K were performed with the DLPOLY code[43] in the canonical ensemble (NVT) using a Nose–Hoover thermostat and periodic boundary conditions. The initial configurations are built with the PACKMOL code[44] providing cubic boxes in which the length of the box sides are chosen to keep a density of 0.997 g/cm^3. In each of the simulations performed, the box contains a phtalocyanine complex fully solvated (several hydration layers before reaching box end). The number of water molecules included are 1398, 1401, and 2085 for the CuPc, H_2Pc, and $[CuPc(SO_3)_4]^{4-}$ systems, respectively. A timestep of 0.5 fs was employed and simulation runs lasted for 10 ns. For the trajectory analysis, structures were saved every 50 timesteps. A cutoff distance of 9 Å was applied in all the cases and Ewald sum methodology[45] applied to account for the electrostatic interactions. For the case of the charged complex, the charged system term has been taken into account.[46] Simulations containing just the amount of water molecules above-mentioned were also performed with the aim of obtaining hydration energies in the energetic analysis (Sec. III).

III. RESULTS

The hydration phenomenon for the considered macrocycles is studied from the structural and energetic point of view on the basis of the molecular dynamics simulations results. The ultimate goal is shedding light on the effects that chemical changes present when moving from one compound to another have on their solvation properties.

A. Energetics

Hydration energies have been computed for the three complexes taking into account the average interaction energies of the simulations involving the complex in solution and the corresponding box containing just the same number of water molecules,

$$\Delta E_{hyd}^{300K} = \langle E_{solute+solvent}\rangle - \langle E_{solvent}\rangle - \langle E_{solute}\rangle. \quad (5)$$

Given that H_2Pc and CuPc have been assumed to be rigid, $E_{solute} = 0$. Then, its average in the above equation is also zero. In the case of $CuPc(SO_3)_4^{4-}$, $\langle E_{solute}\rangle$ represents the average energy of the solute in gas phase at 300 K. The term $\Delta(PV)$ connecting the hydration energy with the experimental hydration enthalpy has been estimated from NPT (isothermal-isobaric ensemble) test simulations for the nonsulphonated systems. Values below 0.5 kcal/mol have been obtained. This means that Eq. (5) provides a fair estimation of the hydration enthalpy.

Values are collected in Table III. Hydration enthalpies for the nonsulphonated complexes are very similar taking into account the error bar estimations (a standard deviation of about

Author complimentary copy. Redistribution subject to AIP license or copyright, see http://jcp.aip.org/jcp/copyright.jsp

TABLE III. Hydration energies (kcal/mol).

Complex	ΔE_{hyd}^{300K}
CuPc	–60
H_2Pc	–51
$CuPc(SO_3)_4^{4-}$	–364

60 kcal/mol is found for each average value). Experimentally the two compounds are highly insoluble in water compared to the highly soluble $CuPc(SO_3)_4^{4-}$ macrocycle that incorporates the water solubilizing sulphonate groups. The tendency is well reproduced by our simulations. Even more, it is known[33,47] that the inclusion of metal ions at the center of the macrocycle, slightly increases its original solubility. Our results also point out in that direction. Values of Table III might lead to think that CuPc and H_2Pc complexes are soluble in water, however two facts hampers that conclusion. The well known tendency to self-aggregate these kind of complexes exhibit[20] leads to take into account a magnitude that must be overcome during the solvation process, i.e., the lattice energy of the solid compound. For the H_2Pc species, the value for that magnitude is found[17] to be in the range [–45.5, –43.6] kcal/mol, i.e., very close to the ΔH_{hyd} values obtained through the simulations. That match leads to think that not only the enthalpic contribution is the driving force for the solvation process, but also the entropic term could play a key role, particularly considering the size of the macrocycle and the solvent reorganization it might imply. However, estimation of the configurational entropy from the simulations is out of the scope of this contribution. The overall impression of the energetic analysis is that the intermolecular potentials employed provide very reasonable and consistent results supporting a detailed analysis of the hydration structure adopted by the solvent around the three different phtalocyanine complexes.

B. Solvent structure

The knowledge of the hydration structure around the complexes should help in understanding the similar or different behavior that the three complexes exhibit in solution. The lack of experimental knowledge about the hydration phenomenon for this kind of macrocycles is remarkable and only understandable for those complexes presenting very low solubility. Therefore the possibility of performing statistical simulations employing reliable interaction potentials become a very attractive alternative because they are able to provide a detailed image of the solvent properties.

A typical function providing information about the distribution adopted by the solvent around a solute is the radial distribution function[45] ($g(r)$). Figure 7 shows the radial distribution functions corresponding to the center of the macrocycle–water oxygen pairs obtained for the three studied cases. For the copper complexes, the RDFs (radial distribution functions) represent the g_{Cu-O} distributions due to the position occupied by the ion in the complex. The three distributions show similar, but not exact, patterns.

In all the cases a well structured distribution can be observed, even at distances as large as 9 Å. Additionally, the first well defined peaks show intensities below one. It is obvious that the size of the complex is in the source of that situation because highly charged (+3) cations,[48–50] for instance, exhibit metal-oxygen distributions that already reaches the limiting value of one at about 8 Å. In fact, the size and the planar symmetry of the macrocycles make RDFs difficult to interpret. One option to overcome this problem could be the analysis of different RDFs centered on different atoms/centers

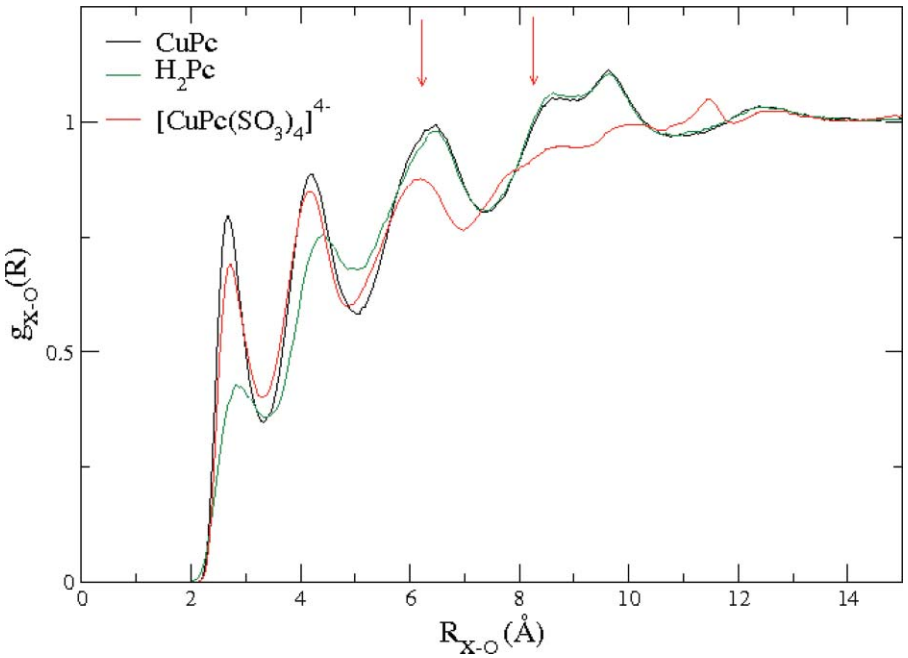

FIG. 7. X–O radial distribution funtions (X = center of the macrocycle) for CuPc (black line), H_2Pc (green line), and $[CuPc(SO_3)_4]^{4-}$ (red line) in water. Arrows locate the average Cu–S distances in the tetrasulphonated complex.

Author complimentary copy. Redistribution subject to AIP license or copyright, see http://jcp.aip.org/jcp/copyright.jsp

of the complexes. Instead, we have adopted a different strategy to study the solvent structure around the solute with the hope of providing a more global view of the changes observed in the solvent distribution for the different macrocycles. On one hand the RDFs of Fig. 7 can be decomposed into contributions obtained for different nonoverlapping regions by an angular definition. In these angular DFs (distribution functions), the space around the central position, geometrical center of the macrocycle in our case, is split into different regions, which are defined by an azimuthal angle θ relative to the axis perpendicular to the molecular plane.[38] This way, distribution functions, equivalent to the global RDF, for the solvent present in each of these regions can be obtained separately. A global, but not spherically averaged, view of the solvent distribution can be obtained by means of spatial distribution functions (SDFs).[51] SDFs show three-dimensional views of the solvation by enclosing volumes in which solvent probability is the highest. Figures used in this work shows volumes enclosing regions where the solvent atom densities are 3.5 times the average solvent density. The discussion of the solvent arrangements around the three studied phthalocyanine complexes will be based on the analysis of these two complementary functions.

1. CuPc

Cu–O and Cu–H RDFs are plotted in Fig. 8. A first peak located at 2.68 Å is found for the Cu–O case while this value moves to 3.07 Å for the Cu–H one. This first shell of oxygen atoms around the copper ion integrates to 1.9 atoms, i.e., almost two water molecules on average are placed in the neighborhood of the metal center. According to the planar character of the macrocycle, they occupy equivalent places but on different sides of the molecular plane. The distance between the water oxygen and hydrogen first maxima (0.39 Å) is a clear indication that the metal center does not impose a marked orientation for those water molecules. For highly oriented water molecules following an ion–dipole interaction,[49] that value is near 0.7 Å. This tendency has already been observed in solvent molecules axially hydrating Pd(II) and Pt(II) square planar hydrated ions[29,38,52] and understood on the basis of the hydrogen-bonded network defined by the rest of solvent molecules. The previous planar complexes were hydrophilic (aquaions) while now the complex is neutral and of hydrophobic character, and interestingly in both the cases a labile situation is found for the water molecules located in that region. Water orientation will be revisited later on the light of the spatial distribution functions.

Well defined peaks, beyond the first shell around the metal center, are found in the Cu–O RDF at 4.2, 6.4, and 8.7–9.6 Å. Whether these peaks define water molecules interacting with other atoms of the macrocycle or belong to bulk water molecules at longer distances of the copper atom is a piece of information not available from that spherically averaged distribution. Angle-resolved distributions can provide such information. Figure 9 shows the decomposition of the Cu–O RDF for three intervals of the θ angle. The interval [0°–30°] defines the first peak centered at 2.68 Å, i.e., the two axial water molecules, and part of the third maximum in Fig. 8 (6.4 Å) which corresponds to solvent molecules in a second axial hydration shell. The second defined contribution in the global RDF (4.2 Å) is defined by water molecules located in the interval [30°–60°]. In particular, that peak is almost exclusively built over water molecule contributions in a more restricted region, [30°–50°], as can be observed in the inset present in Fig. 9. Those water molecules (about six) are essentially hydrogen bonded to the two axial waters previously mentioned. The broad maxima found in the 8.7–9.6 Å

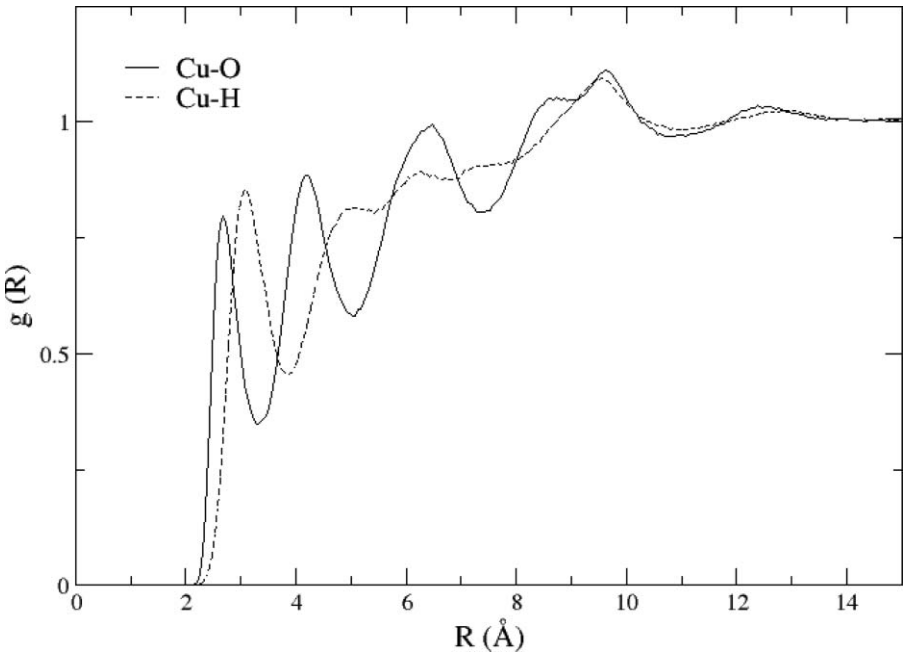

FIG. 8. Cu–O (solid line) and Cu–H (dashed line) radial distribution functions for CuPc in water.

Author complimentary copy. Redistribution subject to AIP license or copyright, see http://jcp.aip.org/jcp/copyright.jsp

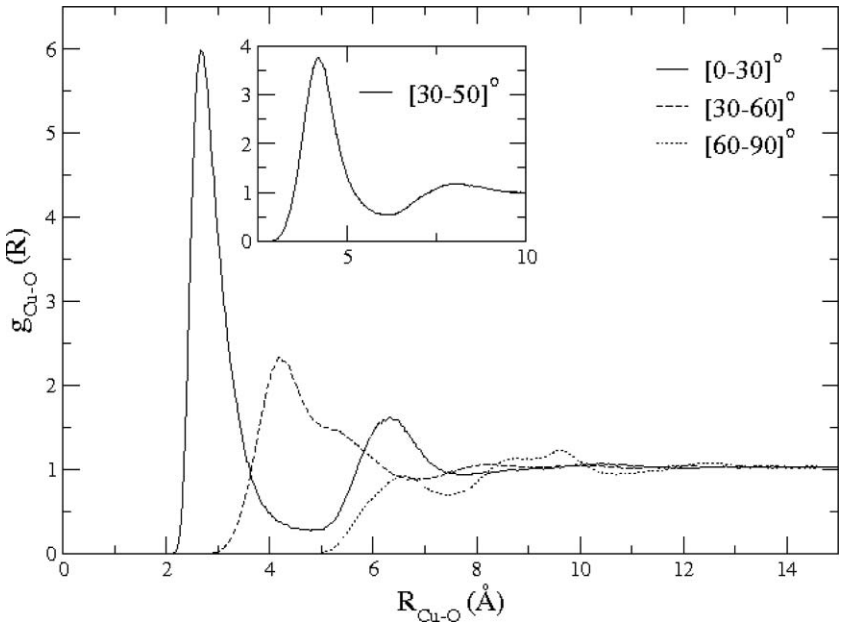

FIG. 9. Decomposition of Cu–O global radial distribution functions for CuPc in water into three angular regions, axial region: $\theta \in [0,30]^\circ$, intermediate region: $\theta \in [30,60]^\circ$, and equatorial region: $\theta \in [60,90]^\circ$. Inset shows the angular distribution function for the region $[30,50]^\circ$.

region are based on the contributions of water molecules near the equatorial region, [60°–90°], and belong therefore to solvent molecules interacting with other atoms of the macrocycle beyond the central copper. Part of the maximum at 6.4 Å is also based on water molecules found in this region. Images of a randomly taken snapshot from the simulation are shown in Fig. 10, where water molecules belonging to the three different regions can be identified.

The Cu–H RDF is much less defined than the Cu–O one, and only the first maximum already mentioned is well resolved. Either orientations imposed by water hydrogen bond network and/or low reorientational times of the water molecules can justify the loss of structure for the water hydrogen distribution.

As previously mentioned, a global and complementary analysis of the solvent distribution can be obtained from the inspection of the SDFs. Figure 11 shows the water oxygen and hydrogen distributions obtained from the analysis of the CuPc simulation for water molecules in the neighborhood of the complex. The oxygen and hydrogen surfaces closest to the

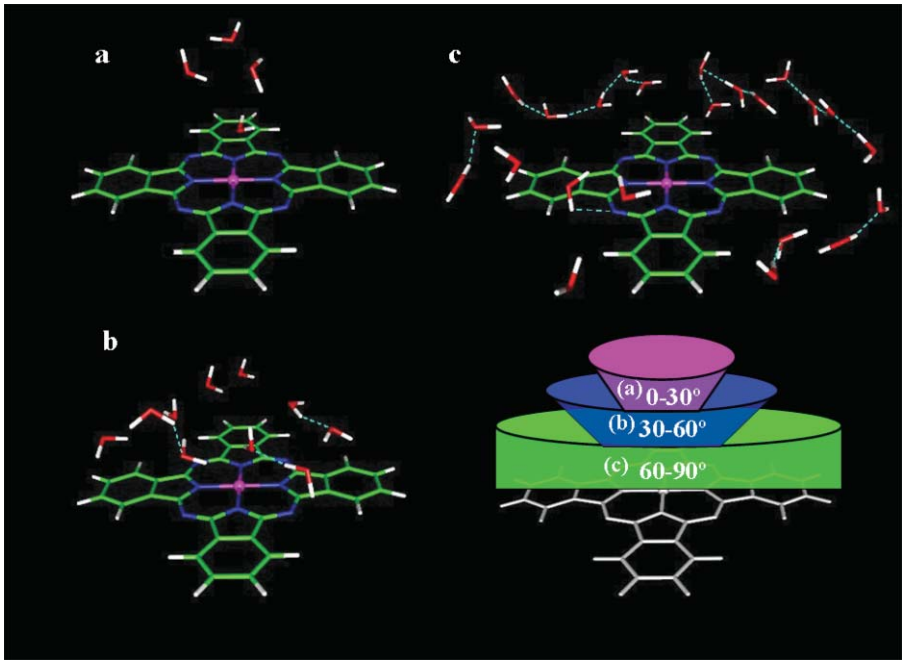

FIG. 10. Snapshot from the simulation CuPc in water. (a) Axial region: $\theta \in [0,30]^\circ$, (b) Intermediate region: $\theta \in [30,60]^\circ$, and (c) Equatorial region: $\theta \in [60,90]^\circ$.

Author complimentary copy. Redistribution subject to AIP license or copyright, see http://jcp.aip.org/jcp/copyright.jsp

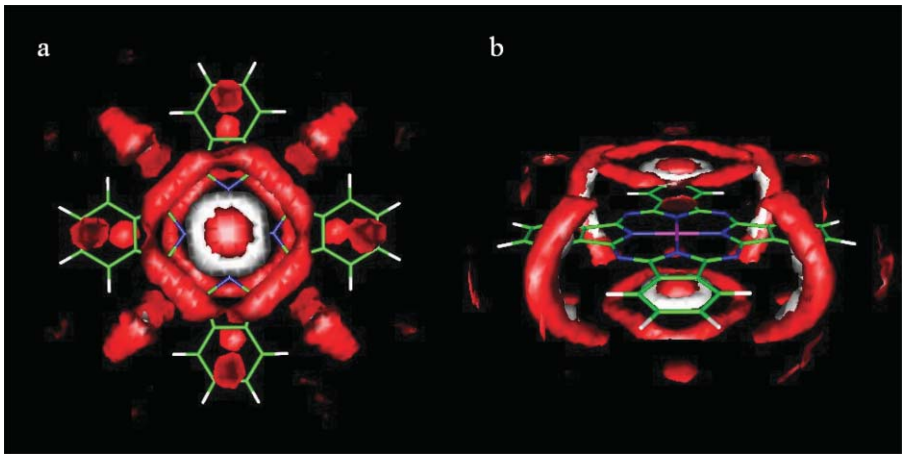

FIG. 11. Water oxygen (red surface) and hydrogen (white surface) SDFs from the simulation of CuPc in water. (a) axial perspective and (b) equatorial perspective.

copper atom are placed in a parallel plane to the macrocycle one, showing a rather parallel orientation of the axial water molecule regarding the complex. Oxygen atoms of the water molecules interacting with them clearly define a ring at the same distance of the complex while hydrogen atoms belonging to both kinds of solvent molecules are clearly placed in between the two oxygen surfaces. This distribution reflects a well structured hydrogen bonded network for the solvent occuppying that region. Other regions exhibiting high solvent density correspond to water molecules located in between the isoindole units which define lobes connecting waters on both sides of the complex plane. It is interesting that for those water molecules, hydrogen and oxygen surfaces coincide what necessarily supposes a sequence of hydrogen bonds spatially adapted to the shape defined by the lobes. The last region with a high density of solvent molecules correspond to molecules located on top (both sides) of the hexagonal ring of the isoindole units. While the red spots are well defined, the lack of high density surfaces associated to the hydrogen atoms denote a region with an easy reorientation for the solvent molecules.

2. H_2Pc and $[CuPc(SO_3)_4]^{4-}$

The way solvent interacts with the other two considered complexes can be analysed on the basis of the differences observed when compared with the CuPc case. In this sense, and paradoxically–considering what previously presented about the global RDFs—Fig. 7 is very informative. The distribution for the H_2Pc complex differs for distances below 6.0 Å, while for longer distances both distributions practically match. In the other complex the situation is simply the opposite, distributions are pretty much the same up to 5.9 Å, while clearly differ for longer distances. In this sense, the free metal Pc and the sulphonated cases exhibit different solvent distributions when compared to the copper phthalocyanine, that correspond to complementary spatial domains. Therefore the analysis concerning these two macrocycles can be focused on those local regions where the differences are observed.

An easy way to confirm this interpretation of the global RDFs is to visualize the differences between SDFs of the solvent atoms obtained for each of the complexes and that of the CuPc. Figure 12 shows the SDF-difference for the metal free phthalocyanine and only those regions

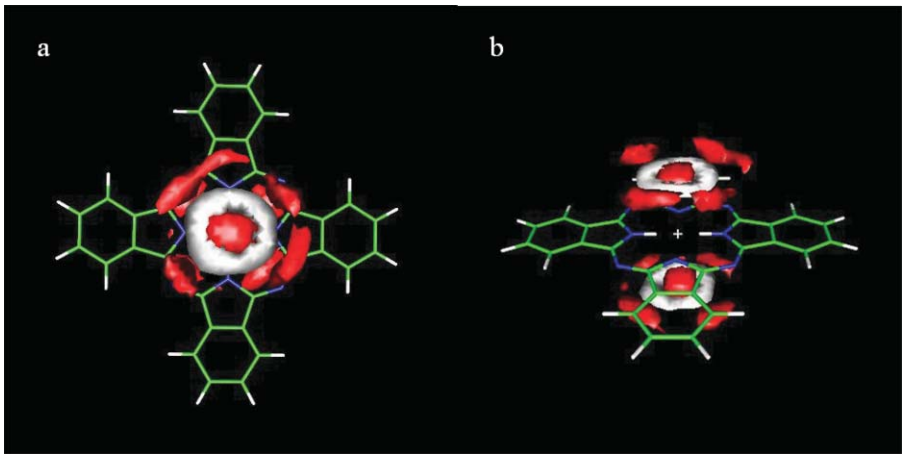

FIG. 12. Solvent SDFs-difference between the CuPc and the H_2Pc simulations (SDF_{CuPc}–SDF_{H_2Pc}). (a) Axial perspective and (b) Equatorial perspective.

Author complimentary copy. Redistribution subject to AIP license or copyright, see http://jcp.aip.org/jcp/copyright.jsp

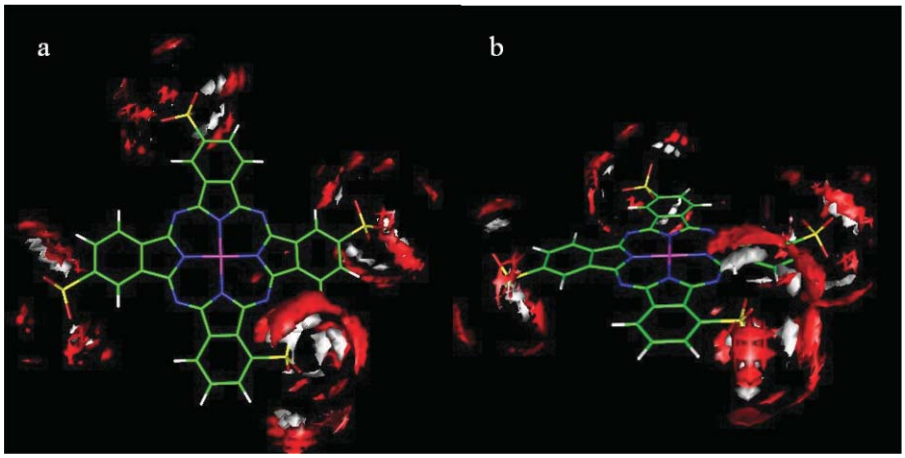

FIG. 13. Solvent SDFs-difference between the $[CuPc(SO_3)_4]^{4-}$ and the CuPc simulations ($SDF_{[CuPc(SO_3)_4]^{4-}} - SDF_{CuPc}$). (a) Axial perspective and (b) Equatorial perspective.

in which the CuPc density is significatively higher are visualized. It is clearly confirmed how the substitution of the copper atom by two hydrogen atoms in the center of the macrocycle makes the axial region to be less populated: the integration number for the tiny RDF peak attributed to the first axial water molecules become now 1.1, defining therefore a more labile solvent structure. Partially, this fact is also transmitted to the solvent molecules directly interacting with those waters as indicated by the nearby spots.

In the $[CuPc(SO_3)_4]^{4-}$ case, the solvent density for distances to the center of the complex in the region 5.8 –10.5 Å is lower than that in the case of the CuPc. It is worth recalling that in that range is where the four centers of the sulphonate groups are located: Cu–S distances of 6.2 Å and 8.2 Å for the nonequivalent and equivalent sulphonates, respectively (small arrows in Fig. 7). It is then easy to understand the decrease of solvent density at those distances of the macrocycle geometrical center. The SDF-difference map for this complex, Fig. 13, shows the hydration shell of the sulphonates where the solvent density is higher compared to the previous phthalocyanines. In fact, on average, each sulphonate is hydrated by eight water molecules which define the last peak (centered at 11.5 Å) of the global Cu–O RDF. Interestingly, Fig. 13 shows two different distributions: one for the three equivalent SO_3^- units and a different, and better defined one, for the nonequivalent group.

In the case of the three equivalent sulphonates (linked to carbon 4 in the isoindol unit), these groups are able to rotate during the simulation, producing a more spherically averaged solvent distribution for the hydration water molecules. In the case of sulphonate group linked to carbon 3, the SDF-difference reflects the more rigid orientation this unit keeps during the whole simulation. Figure 14 shows the distribution of angles adopted by the two type of sulphonates using one O–S–C–C dihedral angle as a reference. Three minima equally populated are found for the equivalent sulphonates with residence times on each minima in the order of 100–200 ps. In contrast, the nonequivalent sulphonate exhibits a hindered rotation keeping one of the equivalent configurations along the simulation with small fluctuations ($\pm 10^\circ$) around it.

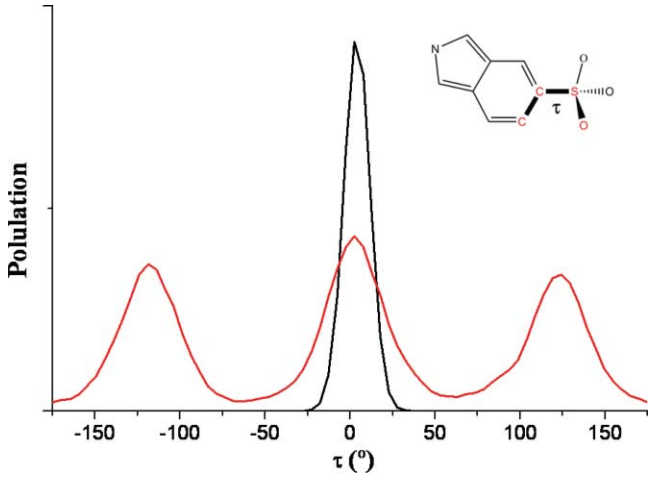

FIG. 14. Population of O–S–C–C dihedral angle of sulphonate groups linked to carbon 4 (red line) or linked to carbon 3 (black line) in the isoindol unit.

3. Experimental detection of hydrating water molecules

Extended x-ray absorption fine structure (EXAFS)[53] spectroscopy is one of the most appropriate techniques to characterize solute environments in dilute aqueous solutions and has also been applied to phthalocyanine complexes.[54] In the most simple case (single scattering analysis), contributions from the atoms surrounding the absorber (copper ion in our case) to the EXAFS signal are summed up by shells (j) of equivalent backscatterer atoms according to the expression[53]

$$\chi(k) = \sum_{\mathrm{j}} \frac{N_{\mathrm{j}} S_o^2}{k \bar{R}_{\mathrm{j}}^2} \left| f_{\mathrm{j}}^{\mathrm{eff}}(k) \right| \sin(2k\bar{R}_{\mathrm{j}} + \varphi(k)) \times e^{-2\bar{R}_{\mathrm{j}}/\lambda(k)} e^{-2\sigma_{\mathrm{j}}^2 k^2}, \quad (6)$$

k being the photoelectron wavevector, that is, the energy of the ejected photoelectron. Each contribution can be understood as an oscillatory signal multiplied by an amplitude factor. For each shell, the simulation analysis yields straightforward estimations for all the following parameters:

Author complimentary copy. Redistribution subject to AIP license or copyright, see http://jcp.aip.org/jcp/copyright.jsp

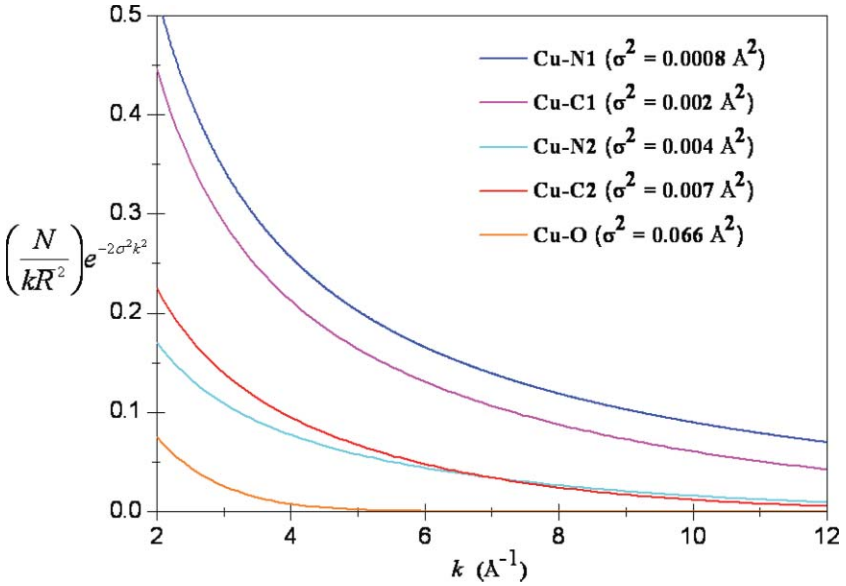

FIG. 15. The envelopes for N1, C1, N2, C2, and axial water oxygen atoms around the copper atom for $[CuPc(SO_3)_4]^{4-}$ in water.

N : number of equivalent atoms in a given shell,
$\bar{R}$: average distance to the absorber for the atoms defining a shell, and
σ : Debye–Waller factor that measures the thermal and structural disorder in a shell.

In principle, the envelope of the oscillatory signal contribution of each shell,

$$\frac{N}{k\bar{R}^2}e^{-2\sigma^2k^2}, \tag{7}$$

can be computed directly from the simulation. Although some factors present in Eq. (6) are not taken into account, the main differences between the different shell contributions are located in the above envelope, specially if the atomic number of the backscatterers are very close, as is our case: N and C atoms around the copper in the complex and O from the solvent. Due to the fact of using a rigid model for the phthalocyanine complexes, we can not estimate σ values for N and C contributions. However, the soluble 3,4′,4″,4‴-tetrasodiumtetrasulphonate phthalocyanine, i.e., one of the complexes here simulated, has been studied by EXAFS in dilute aqueous solutions analyzing the copper K-edge.[55] That work provides structural information such as distances and Debye–Waller factors for the first nitrogen and carbon atoms around the copper center. On the contrary, such information can be obtained for the solvent molecules by analyzing the waters occupying the axial positions during our simulation. Using both, the experimental and theoretical estimations, the envelopes [Eq. (7)] for the nearest atoms around the copper have been built and plotted in Fig. 15. It is clear the marginal contribution that the water oxygen atoms have on the final amplitude. According to this simple analysis, the detection of water molecules in the neighborhood of the copper ion is revealed as a very challenging aim, particularly if one takes into account other relevant contributions arising from multiple scattering phenomena.[55] Our results agrees with the experimental EXAFS analysis as the fit of the experimental signal performed in that case did not improve if axial contributions arising from the solvent molecules were included.

IV. CONCLUSIONS

This work has presented a novel procedure to develop intermolecular potentials between water and a set of phthalocyanine derivatives, based on first-principles quantum mechanical information. The extensive prospection of potential energy surfaces together with the functional form proposed have allowed us to straightforwardly describe an intermolecular potential where the most stabilizing water–phthalocyanine interaction energy is as small as ca. –6.0 kcal/mol. It has been possible due to the small standard deviation obtained in the global fitting, smaller than 0.7 kcal/mol for the case of CuPc. The study of these macrocyles has allowed us to find an operative way to transfer a significant fraction of the intermolecular potential in solution. A transferability procedure has been established to develop a water–phthalocyanine derivative potential. This fact may be considered as the first step for future studies of a wide series of Pcs where new, central or peripheral, functional groups are considered. Furthermore, the proposed method could be easily applied to other families of macrocycles such as porphyrins.

The estimation of the mean interaction energy of insoluble CuPc and H_2Pc, and the soluble $[CuPc(SO_3)_4]^{4-}$ in water, is coherent with the experimental behavior. Interestingly, the analysis of the surrounding solvent structure for the three compounds does not show as dramatic changes as may be expected from their different solubility character. The transition from H_2Pc to CuPc decreases the solvent density located near by the macrocycle center, while the rest of the solvent distribution is not altered by this fact. When the sulphonate groups are introduced in the copper phthalocyanine the changes exclusively affect the water molecules located in the periphery of the macrocycle, the axial region remaining unaltered. The local character of the solute-solvent interaction changes induced by the chemical

Author complimentary copy. Redistribution subject to AIP license or copyright, see http://jcp.aip.org/jcp/copyright.jsp

differences of the macrocycles is a relevant finding. Properties located at the metal center, such as the photosensitizer activity of the complex in solution, should not be affected by the introduction of peripheral solubilizing groups.

The weakly bound axial solvent molecules present structural properties similar to those observed in other—highly soluble—planar complexes such as Pd(II) and Pt(II) hydrated ions.[29,52] Such molecules define in that case what is called *meso-shell*,[29] exhibiting properties in between those found for the first and second hydration shells of a highly charged cation. In the cases here studied the term meso-shell does not apply because they strictly define the first solvent shell around the copper ion. However, this result opens a question: how important is the chemical nature of the planar complex when defining the properties of the water molecules directly interacting with the metal center? Further works on the characterization of the dynamic properties of the solvent interacting with the Pc complexes are currently ongoing.

Finally, the structural analysis performed, and conclusions obtained, reveals angular distribution and spatial distribution functions as very suitable tools to analyze changes in nonradially defined solvent distributions.

ACKNOWLEDGMENTS

Financial support from the Ministerio de Ciencia e Innovacion (CTQ2008-05277) is acknowledged. E.I.M. thanks to the Spanish Ministerio de Educacion for a predoctoral FPI grant.

[1] T. J. Dougherty, C. J. Gomer, B. W. Henderson, G. Jori, D. Kessel, M. Lorbelik, J. Moan, and Q. Peng, J. Natl. Cancer Inst. **90**, 889 (1998).
[2] S. B. Brown, E. A. Brown, and I. Walker, Lancet Oncol. **5**, 497 (2004).
[3] R. R. Allison, G. H. Downie, R. Cuenca, X. H. Hu, C. J. Childs, and C. H. Sibata, Photodiagn. Photodyn. Ther. **1**, 27 (2004).
[4] M. R. Betty, S. L. Gibson, and S. J. Wagner, J. Med. Chem. **47**, 3897 (2004).
[5] N. L. Oleinick, A. R. Antunez, M. E. Clay, B. D. Rihter, and M. E. Kenney, Photochem. Photobiol. **57**, 242 (1993).
[6] R. K. Pandey, J. Porphyr. Phthalocyanines **4**, 368 (2000).
[7] C. M. Allen, W. M. Sharman, and J. E. Van-Lier, J. Porphyr. Phthalocyanines **5**, 161 (2001).
[8] I. J. Macdonald and T. J. Dougherty, J. Porphyr. Phthalocyanines **5**, 105 (2001).
[9] S. L. Haywood-Small, D. I. Vernon, J. Griffiths, J. Schofield, and S. B. Brown, Biochem. Biophys. Res. Commun. **339**, 569 (2006).
[10] M. S. Xu, J. B. Xu, M. Wang, and L. Que, Appl. Phys. **91**, 748 (2002).
[11] L. E. Norena-Franco and F. K. Vasnik, Analyst (Amsterdam) **121**, 1115 (1996).
[12] A. Hagfeldt and M. Gratzel, Acc. Chem. Res. **33**, 269 (2000).
[13] M. Calvete, G. Y. Yang, and M. Hanack, Synth. Met. **141**, 231 (2004).
[14] R. Bonnett, *Chemical Aspects of Photodynamic Therapy* (Gordon and Breach Science Publishers, Amsterdam, 2000).
[15] *Phthalocryanine: Properties and Applications*, edited by C. C. Leznoff and A. B. P. Lever (VCH Publishers, Germany, 1989).
[16] N. B. McKeown, *Phthalocyanine Materials: Synthesis Structure and Function* (Cambridge University Press, Cambridge, 1998).
[17] R. B. Hammond, K. J. Roberts, R. Docherty, M. Edmondson, and R. Gairns, J. Chem. Soc., Perkin Trans. **2**, 1527 (1996).
[18] S. Yim, S. Heutz, and T. S. Jones, Phys. Rev. B **67**, 165308 (2003).
[19] M. C. DeRosa and R. J. Crutchley, Coord. Chem. Rev. **233**, 351 (2002)
[20] T. Nyokong, Coord. Chem. Rev. **251**, 1707 (2007).
[21] Y. Chen, M. Hanack, W. J. Blau, D. Dini, Y. Liu, Y. Lin, and J. Bai, J. Mater. Sci. **41**, 2169 (2006).
[22] M. Durmuş and T. Nyokong, Photochem. Photobiol. Sci. **6**, 659 (2007).
[23] V. Chauke, A. Ogunsipe, M. Durmuş, and T. Nyokong, Polyhedron **26**, 2663 (2007).
[24] M. Idowu and T. Nyokong, J. Photochem. Photobiol. A: Chem. **199**, 282 (2008).
[25] D. K. Modibane and T. Nyokong, Polyhedron **27**, 1102 (2008).
[26] J. F. Fuchs, H. Nedev, D. Poger, M. Ferrand, V. Brenner, J. P. Dognon, and S. Crouzy, J. Comput. Chem. **27**, 837 (2006).
[27] R. R. Pappalardo and E. Sánchez Marcos, J. Phys. Chem. **97**, 4500 (1993).
[28] R. R. Pappalardo, J. M. Martínez, and E. Sánchez Marcos, J. Phys. Chem. **100**, 11748 (1996).
[29] J. M. Martínez, F. Torrico, R. R. Pappalardo, and E. Sánchez Marcos, J. Phys. Chem. B **108**, 15851 (2004).
[30] See supplementary material at http://dx.doi.org/10.1063/1.3528934 for fitted coefficients and charges of the different intermolecular potentials developed in this work.
[31] F. Evangelista, V. Carravetta, G. Stefani, B. Jansik, M. Alagia, S. Stranges, and A. Ruocco, J. Chem. Phys. **126**, 124709 (2007).
[32] M. J. Frisch, G. W. Trucks, H. B. Schlegel, G. E. Scuseria, M. A. Robb, J. R. Cheeseman, J. J. A. Montgomery, T. Vreven, K. N. Kudin, J. C. Burant, J. M. Millam, S. S. Iyengar, J. Tomasi, V. Barone, B. Mennucci, M. Cossi, G. Scalmani, N. Rega, G. A. Petersson, H. Nakatsuji, M. Hada, M. Ehara, K. Toyota, R. Fukuda, J. Hasegawa, M. Ishida, T. Nakajima, Y. Honda, O. Kitao, H. Nakai, M. Klene, X. Li, J. E. Knox, H. P. Hratchian, J. B. Cross, V. Bakken, C. Adamo, J. Jaramillo, R. Gomperts, R. E. Stratmann, O. Yazyev, A. J. Austin, R. Cammi, C. Pomelli, J. W. Ochterski, P. Y. Ayala, K. Morokuma, G. A. Voth, P. Salvador, J. J. Dannenberg, V. G. Zakrzewski, S. Dapprich, A. D. Daniels, M. C. Strain, O. Farkas, D. K. Malick, A. D. Rabuck, K. Raghavachari, J. B. Foresman, J. V. Ortiz, Q. Cui, A. G. Baboul, S. Clifford, J. Cioslowski, B. B. Stefanov, G. Liu, A. Liashenko, P. Piskorz, I. Komaromi, R. L. Martin, D. J. Fox, T. Keith, M. A. Al-Laham, C. Y. Peng, A. Nanayakkara, M. Challacombe, P. M. W. Gill, B. Johnson, W. Chen, M. W. Wong, C. Gonzalez, and J. A. Pople, GAUSSIAN 03 , revision D.01; Gaussian, Inc., Wallingford, CT, 2004.
[33] J. Poater, M. Solá, A. Rimola, L. Rodríguez-Santiago, and M. Sodupe, J. Phys. Chem. A **108**, 6072 (2004).
[34] R. Rios-Font, M. Sodupe, L. Rodríguez-Santiago, and P. R. Taylor, J. Phys. Chem. A **114**, 10857 (2010).
[35] M. J. Elrod and R. J. Saykally, Chem. Rev. **94**, 1975 (1994).
[36] J. R. Alvarez-Idaboy and A. Galano, Theor. Chem. Acc. **126**, 75 (2010).
[37] K. S. Kim, P. Tarakeshwar, and J. Y. Lee, Chem. Rev. **100**, 4145 (2000).
[38] E. C. Beret, J. M. Martínez, R. R. Pappalardo, E. Sanchez Marcos, N. Doltsinis, and D. Marx, J. Chem. Theory Comput. **4**, 2108 (2008).
[39] H. J. C. Berendsen, J. R. Grigera, and T. P. Straatsma, J. Phys. Chem. **91**, 6269 (1987).
[40] B. H. Besler, K. M. Merz, Jr., and P. A. Kollman, J. Comput. Chem. **11**, 431 (1990).
[41] U. C. Singh and P. A. Kollman, J. Comput. Chem. **5**, 129 (1984).
[42] A. D. MacKerell, D. Bashford, M. Bellott, R. L. Dunbrack, Jr., J. D. Evanseck, M. J. Field, S. Fischer, J. Gao, H. Guo, S. H. and D. Joseph-McCarthy, L. Kuchnir, K. Kuczera, F. T. K. Lau, C. Mattos, S. Michnick, T. Ngo, D. T. Nguyen, B. Prodhom, W. E. Reither III, B. Roux, M. Schlenkrich, J. C. Smith, R. Stote, J. Straub, M. Watanabe, J. Wirkiewicz-Kuczera, D. Yin, and M. Karplus, J. Phys. Chem. B **102**, 3586 (1998).
[43] W. Smith and T. Forester, J. Mol. Graphics **14**, 136 (1996).
[44] J. M. Martínez and L. Martínez, J. Comput. Chem. **24**, 819 (2003).
[45] M. P. Allen and D. J. Tildesley, *Computer Simulation of Liquids*. (Clarendon, Oxford, 1989)
[46] K. Refson, Comput. Phys. Commun. **126**, 310 (2000).
[47] Y. Chen, M. Hanack, Y. Araki, and O. Ito, Chem. Soc. Rev. **34**, 517 (2005).
[48] J. M. Martínez, R. R. Pappalardo, and E. Sánchez Marcos, J. Chem. Phys. **109**, 1445 (1998).
[49] J. M. Martínez, R. R. Pappalardo, and E. Sánchez Marcos, J. Am. Chem. Soc. **121**, 3175 (1999).
[50] F. Carrera, F. Torrico, D. T. Richens, A. Munoz-Páez, J. M. Martínez, R. R. Pappalardo, and E. Sánchez Marcos, J. Phys. Chem. B **111**, 8223 (2007).
[51] D. L. Bergman, L. Laaksonen, and A. Laaksonen, J. Mol. Graphics Modell. **15**, 301 (1997).
[52] F. Torrico, R. R. Pappalardo, E. Sánchez Marcos, and J. M. Martínez, Theor. Chem. Acc. **115**, 196 (2006).
[53] D. E. Sayers, E. A. Stern, and F. W. Lytle, Phys. Rev. Lett. **27**, 1204 (1971).
[54] V. Krishnan, M. P. Feth, E. Wendel, Y. Chen, M. Hanack, and H. Bertagnolli, Z. Phys. Chem. **218**, 1 (2004).
[55] F. Carrera, E. Sánchez Marcos, P. J. Merkling, J. Chaboy, and A. Munoz-Páez, Inorg. Chem. **43**, 6674 (2004).

All in-text references underlined in blue are linked to publications on ResearchGate, letting you access and read them immediately.
Author complimentary copy. Redistribution subject to AIP license or copyright, see http://jcp.aip.org/jcp/copyright.jsp